

Volcanic tremor and long period events at Mt. Etna: Same mechanism at different rates or not?

Mariangela Sciutto^{a,*}, Andrea Cannata^{a,b}, Giuseppe Di Grazia^a, Placido Montalto^a

^a Istituto Nazionale di Geofisica e Vulcanologia, Osservatorio Etneo, Piazza Roma, 2, Catania, Italy

^b Dipartimento di Scienze Biologiche, Geologiche e Ambientali, Università Degli Studi di Catania, Piazza Università, 2, Catania, Italy



ARTICLE INFO

Keywords:

Volcanic tremor
Long period events
Mt. Etna
Volcano seismology
Volcano monitoring

ABSTRACT

Volcanic tremor and long period (LP) events are typical seismic signals recorded on active volcanoes and are characterized by different durations, longer than minutes and a few seconds - tens of seconds for the former and latter, respectively. As they share the same frequency content, they are often grouped together in the literature and referred to by the unique name of LP seismicity. The common spectral features, together with observations in some volcanoes of individual LP events merging to form volcanic tremor, led to hypotheses that LP events and volcanic tremor share the same source mechanism. However, it is still open to debate whether volcanic tremor can be considered a simple coalescence of LP events or not. In this work, to help answer such a question, we analysed volcanic tremor and LP events recorded at Mt. Etna during the period February 2019–June 2020, characterized by minor eruptive activity, varying from weak ash emission to explosive and effusive eruptions at all the summit craters. Results from spectral, amplitude and location analyses, as well as the different scaling laws explaining the distributions of the duration/number of events versus size, led us to infer that LP events and volcanic tremor at Mt. Etna are not due to a common source mechanism.

1. Introduction

Volcano seismology, together with geodesy and geochemistry, represents one of the three pillars among the disciplines used in the framework of both volcanic unrest detection and hazard assessment/risk mitigation (Zobin, 2012, and reference therein).

Studies of seismic signals originating in volcanic areas are of crucial importance in volcano monitoring because they are generally related to magmatic and hydrothermal fluids, and to their dynamic interactions with surrounding rocks along magma pathways (e.g., cracks, conduits, opening dikes; e.g., Chouet and Matoza, 2013). Besides volcano-tectonic (VT) earthquakes, which originate from fracturing of volcano rocks with a double-couple source mechanism (Aki and Richards, 2002) mainly due to stresses deriving from magmatic processes (Chouet et al., 1994), a wide range of signals in a lower frequency range (generally <5 Hz) is observed in volcanic areas. These events likely originate in the fluids and represent volumetric modes of deformation involving a localized response of plumbing system portions to flow processes (e.g., Chouet and Matoza, 2013). Processes generating low frequency signals mainly result from magmatic and hydrothermal fluid movement, pressurization of the volcano edifice, surface phenomena (e.g., eruptive activity or

landslides) and interactions among them and geometrical/structural characteristics of the shallow plumbing system (e.g. Wassermann, 2012; Chouet and Matoza, 2013).

Several schemes have been proposed in the literature to classify low frequency seismic signals recorded in volcanic areas, accounting for their waveforms, durations, frequency contents or source mechanisms (e.g. Minakami, 1960; Chouet, 1996; McNutt, 2005; Wassermann, 2012; McNutt and Roman, 2015). Following one of the last reviews in volcano seismology outcomes, McNutt and Roman (2015), apart from VT earthquakes, seismo-volcanic signals can be distinguished in:

- long period (LP) or low frequency (LF) events (originally called B-type volcanic earthquakes), which often have emergent P waves and lack distinct S waves. Under this name are usually classified seismic events with dominant frequencies between 0.5 or 1.0 and 5.0 Hz. They have been mainly associated with fluid pressurization processes, such as bubble formation and collapse, or nonlinear flow processes that occur in rectangular cracks or cylindrical pipes. Even shear failure or tensile failure of the rock have been considered as possible source mechanisms for LP events (Bean et al., 2014);

* Corresponding author.

E-mail address: mariangela.sciutto@ingv.it (M. Sciutto).

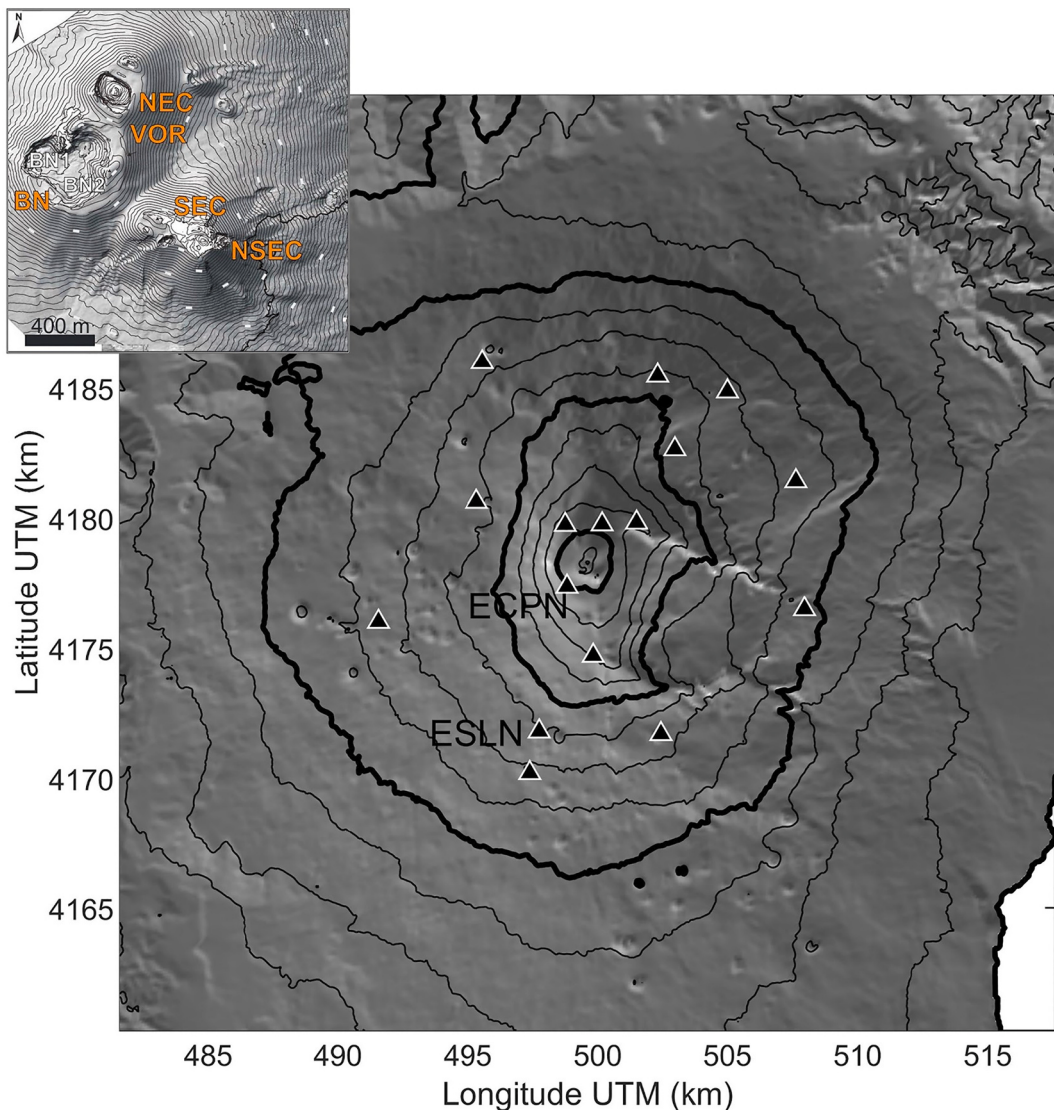


Fig. 1. Digital elevation map of Mt. Etna, showing the location of the seismic stations used to investigate the LP seismicity. The inset in the upper left corner shows the summit area with the main craters (South-East Crater: SEC; New South-East Crater: NSEC; Bocca Nuova: BN; Voragine: VOR; and North-East Crater: NEC; from Neri et al., 2017).

- very long period (VLP) events with periods of 3–50 s, which have been observed in many volcanoes worldwide, thanks to the installation of broadband seismometers in the last two-three decades, that have enhanced our ability to detect ground motions at lower frequencies. To explain the origin of the VLP events, different types of models have been suggested, involving inertial forces associated with perturbations in the flow of magma and gases through conduits (Chouet and Matoza, 2013), such as pressure changes caused by the generation or the ascent of a gas slug in the volcanic conduit of Stromboli (Chouet et al., 2003);
- hybrid events, which are transient signals sharing characteristics of both VT earthquakes and LP events. Their spectrum is made up of high and low frequency peaks, with the higher frequency usually occurring at the onset of the event. The name descends from the source mechanism, that according to the prevailing theories is a mixture of processes such as fracturing phenomena taking place close to a fluid-filled cavity and then setting it into oscillation (Lahr et al., 1994);
- volcanic tremor, which is by far the more intriguing seismic signal recorded at volcanoes, due to its complex and debated source mechanism. Its spectral content varies in the same frequency band as

LP events, but consists of a more continuous vibration of the ground, which can last for minutes, days or even years. It can be monochromatic or broadband (Girona et al., 2019). Together with the variability of its duration, strong amplitude variations are often recognized. Abrupt spectral and amplitude variations are often associated with explosive volcanic activity occurrence, and this kind of signal is named eruptive/eruption tremor (Ichihara, 2016; Gestrich et al., 2020; Haney et al., 2020). At some volcanoes the occurrence of a particular kind of volcanic tremor, characterized by regular cyclic increases of amplitude and called “banded” tremor, has been reported and attributed to hydrothermal flow instability (Fujita, 2008; Cannata et al., 2010). Several mechanisms have been proposed to explain the different kinds of volcanic tremor, including fluid-elastic resonance and frictional processes (Girona et al., 2019 and reference therein);

- explosion-quakes, which are seismic amplitude transients accompanying the explosive eruptions. In this case, since the source is coupled with both solid Earth and atmosphere, the explosion-quakes have both seismic and acoustic components.

Besides this classification scheme, often in literature the short-lived

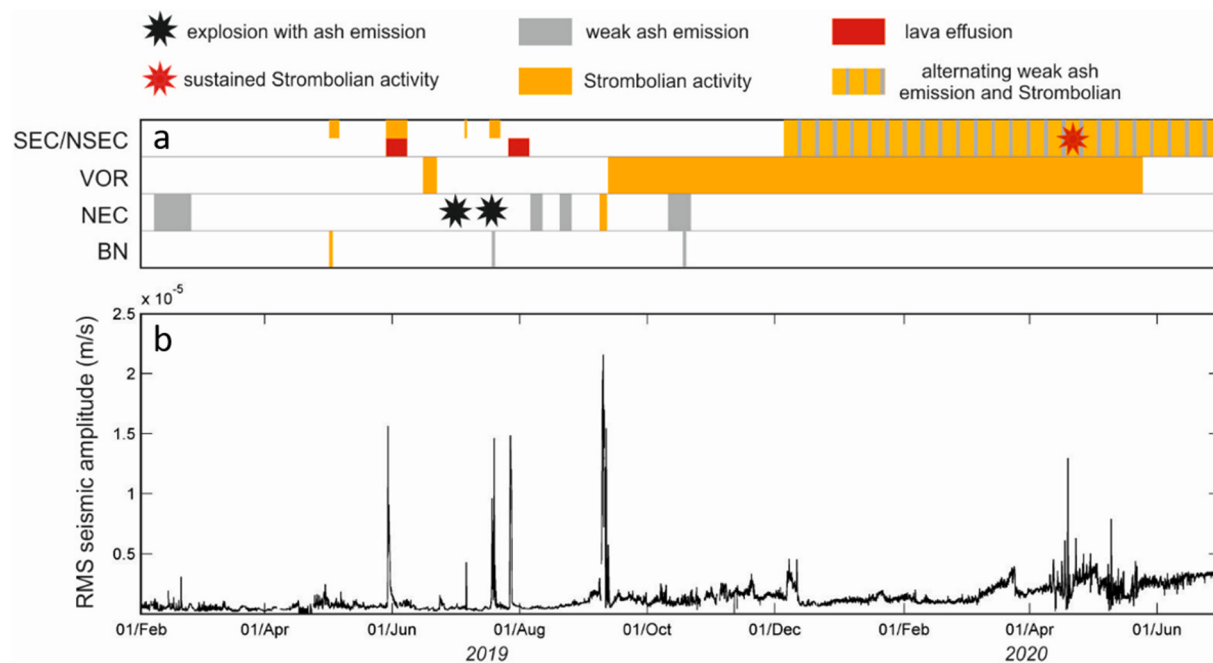


Fig. 2. (a) Sketch showing the eruptive periods at SEC/NSEC, VOR, NEC and BN (see the top legend). (b) RMS amplitude of the seismic signal recorded by the vertical component of ESLN station.

LP events and the longer-duration volcanic tremor are grouped together and referred to the unique name of LP seismicity (Chouet and Matoza, 2013). In a few studies they have been inferred to share the same source mechanism, as these signals roughly share the same frequency content (< 5 Hz), and in some instances individual LP events merge to form volcanic tremor (e.g., Latter, 1979; Fehler, 1983; Neuberg, 2011; Hotovec et al., 2012; Chouet and Matoza, 2013; D'Auria et al., 2019). Nevertheless, other researches, based on the wavefield properties, head towards the hypothesis of a different source process (e.g., Almendros et al., 2014).

However, as highlighted by Chouet and Matoza (2013), volcanic tremor recorded on volcanoes worldwide shows a very wide range of behaviour and, in general, its characteristics in terms of both amplitude and spectral content depend on the volcano eruptive style. Hence, it is still open to debate whether it can be considered a coalescence of LP events or not.

Shedding light into this matter can improve our understanding of the seismicity recorded on volcanoes and hence its interpretation in the perspective of volcano monitoring and surveillance. For instance, on volcanoes where LP events and volcanic tremor are ascribed to the same source mechanism, the LP event occurrence rate can be a very useful parameter to be monitored. Indeed, increases in LP occurrence rate and the successive merging into a continuous tremor have often been observed immediately before explosive volcanic activities (e.g., Popocatepetl, Arciniega-Ceballos et al., 2000; Augustine, Buurman and West, 2010; Redoubt, Buurman et al., 2013). Moreover, if they share the same mechanism, both LP and tremor should have the same meaning in terms of hazard assessment. Conversely, if LP events and tremor have different source mechanisms, their features are expected to change independently and have distinct meaning in terms of volcano monitoring and surveillance. For instance, the LP event rate could be unrelated from the time amplitude pattern of volcanic tremor. This has direct implications for early warning system implementation. Indeed, in some volcanoes, such systems are based only on the variation over time of the volcanic tremor amplitudes and not on the LP event features (e.g., D'Agostino et al., 2013; Potter et al., 2014; Cannavò et al., 2017).

At Mt. Etna (Italy), volcanic tremor and LP events are frequently recorded. One of the main features of the former is its close relationship

to changes in observable volcanic activity, as it has been proved by variations in amplitude, spectral content, wavefield features, and source location, taking place at the same time as changes in activity (e.g., Gresta et al., 1991; Alparone et al., 2007; Patanè et al., 2008; Cannata et al., 2018; Cannavò et al., 2019). Concerning LP events, waveform and spectral features, and in particular their changes over time, are likely to be associated with the conditions of the shallowest portion of the plumbing system (e.g., Patanè et al., 2008; Cannata et al., 2015). For instance, LP spectral changes and amplitude increases have allowed us to recognize the pressurization of the plumbing system before a violent explosion, that occurred at Bocca Nuova crater (BN; Fig. 1) on 5 September 2013, which was then followed by a series of lava fountains (Cannata et al., 2015).

In this paper, we analyze volcanic tremor and LP events in a 17-month-long interval (February 2019–June 2020) with the aim of characterizing their features and tracking down, if there are, differences between them, as well as their temporal patterns and relationships with volcanic activity. The study of the characteristics of the LP seismicity of Mt. Etna helps answer the question of whether volcanic tremor can be considered a coalescence of LP events, and thus shares exactly the same source process, or volcanic tremor and LP events have to be considered as resulting from different mechanisms.

2. Materials and methods

2.1. Volcanological framework

Mt. Etna is considered as one of the most active volcanoes in the world (e.g., Global Volcanism Program, 2013). The frequent eruptive activities can take place from: i) the summit craters; or ii) fissures opened on the volcano flanks or along the low slopes of the summit cones. Concerning the former, since 1986 an increase in the occurrence rate of the mid-intensity explosive eruptions has occurred with more than 240 paroxysmal episodes, characterized by Strombolian and/or lava fountaining activity resulting in eruption columns, from then to 2021 (Andronico et al., 2021). The latter eruptions are less frequent compared to the summit eruptions, and are generally preceded by clear geophysical signatures in terms of VT earthquake swarms and intense

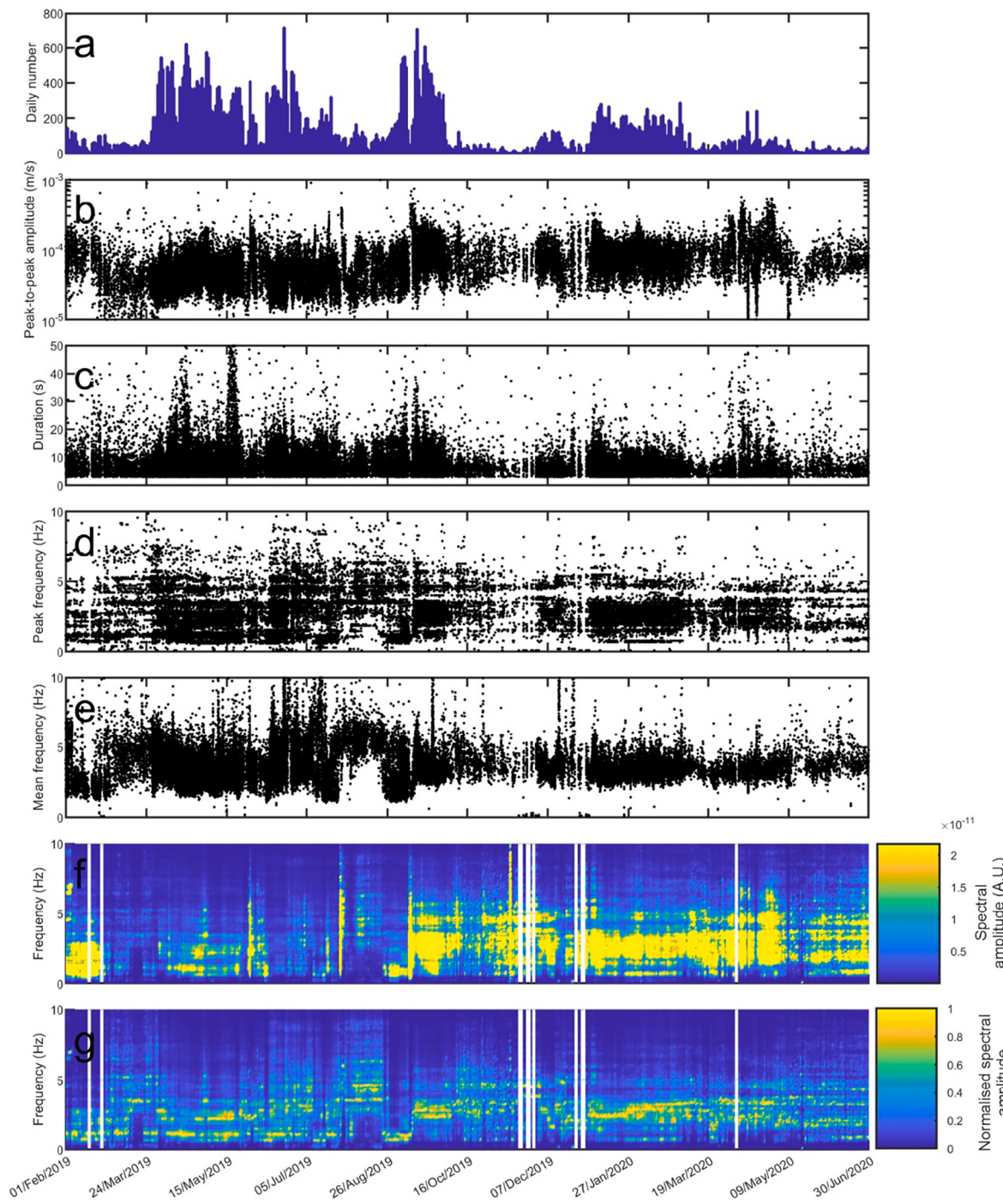


Fig. 3. (a) Daily number of LP events, (b) peak-to-peak amplitude, (c) duration, (d) peak frequency, (e) mean frequency, (f) pseudo-spectrogram and (g) normalised pseudo-spectrogram of the LP events, computed on the signal recorded by the vertical component of station ECPN.

ground deformation, that lack in the summit eruptions (Andronico et al., 2021). One of the most recent flank eruptions took place on 24–27 December 2018 (the so called “Christmas Eve Eruption”) and was accompanied by very intense VT earthquake activity, as well as by evident ground deformation (e.g., Bonforte et al., 2019; Cannavò et al., 2019; Calvari et al., 2020). After this eruption, Mt. Etna experienced a period of intermittent and energetically variable, intra-crateric Strombolian activity and ash emission from the summit craters (mainly from North-East Crater, NEC; Fig. 1) (Giuffrida et al., 2021).

In particular, at NEC, in February 2019 a few explosive episodes producing ash plumes occurred (Fig. 2). In the next 2 months, the Mt.

Etna summit craters were characterized by a weak and ordinary degassing regime, while on the first days of May, sporadic Strombolian activity again resumed at BN Crater and at New South-East Crater (NSEC; Figs. 1 and 2). The area of this crater was the location of multiple episodes of intense Strombolian and effusive activity, both from summit vents and from eruptive fractures that opened on the flanks, such as 30 May–6 June and 27–28 July 2019. As regarding the other summit craters, during the rest of June, July and August, several episodes of explosive activity, impulsive and producing ash emission (on 18–19 July the most energetic one occurred at NEC; Fig. 2) or lasting a few days (Voragine Crater, VOR; Fig. 2), took place. Successively, from the

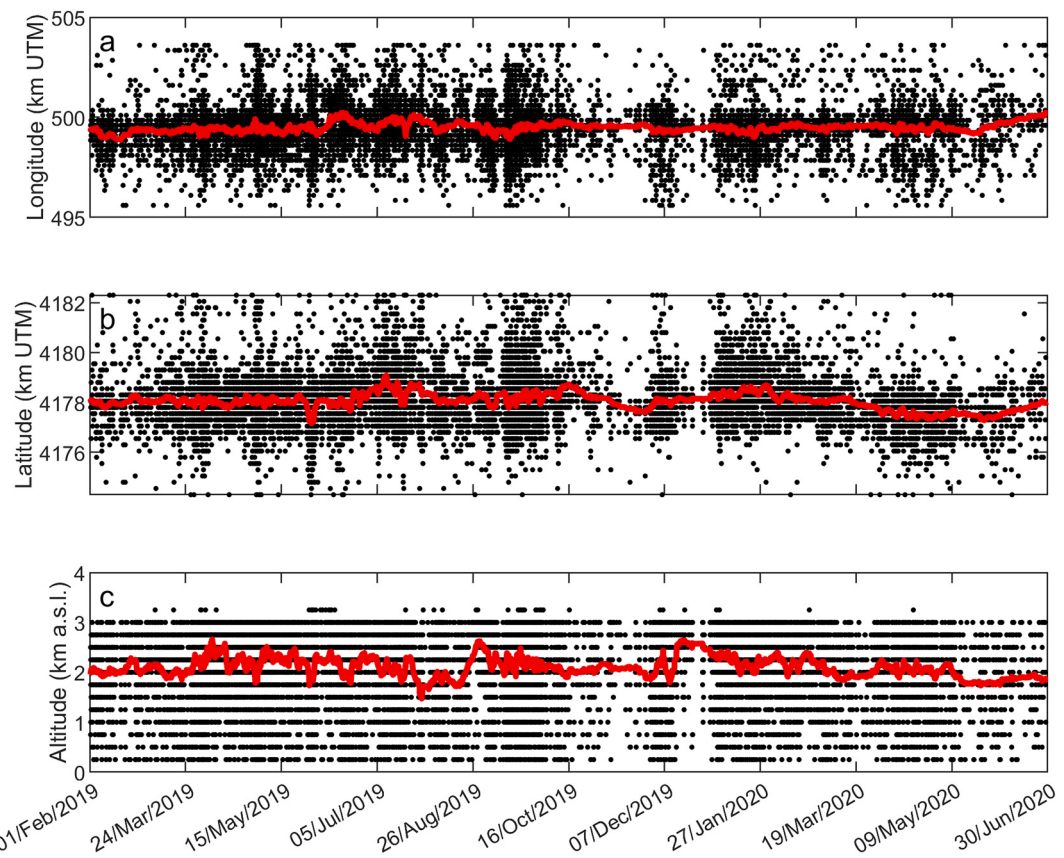


Fig. 4. Variation over time of longitude (a), latitude (b) and altitude (c) of the source locations of LP events (black dots). The thick red lines indicate the moving average time series computed over 100 LP event locations. (For interpretation of the references to colour in this figure legend, the reader is referred to the web version of this article.)

beginning of September and until the end of November 2019, the eruptive activity was mainly located at VOR, where Strombolian activity was almost continuously observed. From about mid-December, together with the activity at VOR, even the South-East and New South-East Crater (SEC/NSEC) area was affected by continuous volcanic phenomena, consisting of an alternation of Strombolian explosions and weak ash emissions. Eruptive activity in this area occurred on 19 April 2020, giving rise to sustained Strombolian activity, then carried on until the end of the period analysed in this work, while at VOR activity ceased at the end of May 2020 (Fig. 2).

2.2. Data

The selected time interval starts from February 2019, after the end of the December 2018 eruption, encompassing a period of minor eruptive activity, varying from weak ash emission to explosive and effusive eruptions at all the Etna summit craters until June 2020. During this interval, different kinds of LP events, with variable occurrence rates, were observed and volcanic tremor experienced two main amplitude increases (Fig. 2). To investigate LP events and volcanic tremor at Mt. Etna, we used seismic signals recorded by 16 stations, belonging to the permanent seismic network run by Istituto Nazionale di Geofisica e Vulcanologia – Osservatorio Etneo (INGV-OE; Fig. 1). The seismic stations are equipped with broadband (40 s cutoff period), three-component Trillium seismometers (Nanometrics™), acquiring in real time at a sampling rate of 100 Hz. In order to find the eventual infrasound component associated with LP events, we used recordings of an infrasound sensor installed at ECPN (co-located with the seismometer; see Fig. 1), which is one of the 10 stations, making up the permanent infrasonic network run by INGV-OE. The sensor is a GRAS 40AN

microphone with a flat response at a sensitivity of 50 mV/Pa in the frequency range of 0.3–20,000 Hz and sampling rate of 50 Hz. Seismic and infrasonic stations transmit the real-time data streaming via satellite or radio to the unified data acquisition center of the INGV-OE located in Catania.

2.3. Methods

As for the LP events, they were automatically detected by the algorithm STA/LTA (short time average/long time average; e.g., Trnkoczy, 2012). To characterise these events, we carried out waveform, spectral and location analyses, as well as visual inspection of the seismograms. The first two analyses were performed by using the signals recorded by ECPN station (Fig. 1), which is routinely considered as the reference station for LP events study at Etna due to its location very close to the usual LP sources (e.g., Cannata et al., 2015). Concerning the waveform features, peak-to-peak amplitude and duration information was extracted, while peak frequency, mean frequency and pseudo-spectrograms were calculated to follow the spectral evolution over time (Fig. 3). The peak frequency is computed as the frequency value with the maximum spectral amplitude, and the mean frequency as the weighted mean of the overall frequency distribution (e.g., Carniel et al., 2005) (Fig. 3d,e). Regarding the pseudo-spectrograms (examples can be found in Spina et al., 2014, and Cannata et al., 2015), they were computed as follows: i) a spectrum was calculated by the Fast Fourier Transform (FFT) algorithm per each LP event on a 10-s-long window, recorded by the vertical component of station ECPN and starting at the onset of the event; ii) the spectra of the events falling in a given day were averaged to obtain a daily average spectrum; iii) all the daily spectra were gathered and visualized with time in the x-axis, frequency in the y-axis, and the

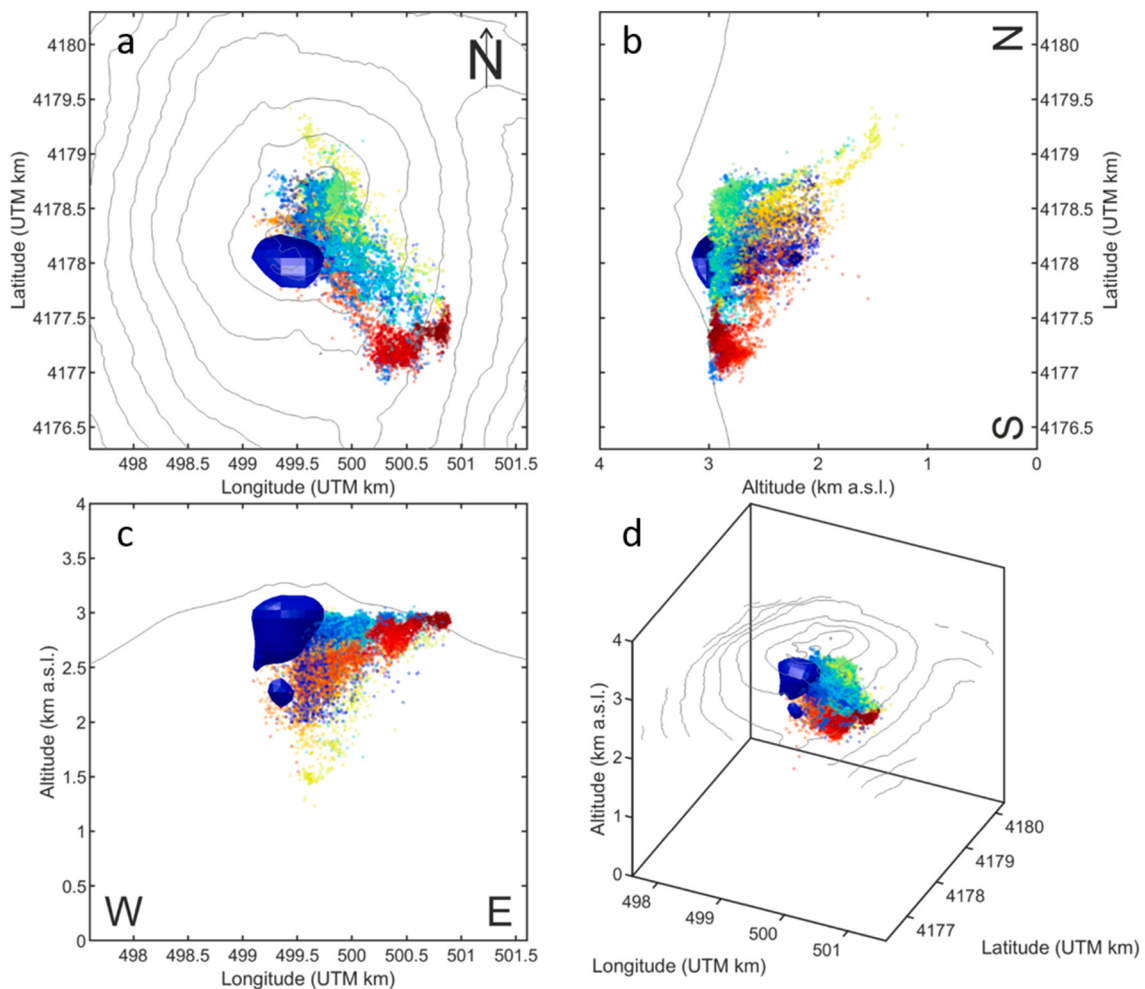


Fig. 5. Map (a), sections (b,c) and 3D view (d) of Mt. Etna showing the locations of LP events (blue surface) and volcanic tremor (colored dots). Regarding LP locations, the blue surface encloses the rock volume, containing location grid nodes with more than 200 LP event locations. As for volcanic tremor, the dot colour depends on the time (see Fig. 6a–d). (For interpretation of the references to colour in this figure legend, the reader is referred to the web version of this article.)

colour scale showing the spectral amplitude (Fig. 3f). Also, the normalised version of the pseudo-spectrogram was computed by dividing each daily spectrum by its maximum value (Fig. 3g).

In addition, information about LP source locations was obtained by a grid-search method based on the computation of two functions: semblance, used to measure the similarity among signals recorded by two or more stations (Neidell and Taner, 1971), and R^2 , calculated on the basis of the spatial distribution of seismic amplitude (see Cannata et al., 2013, for further details; Figs. 4 and 5). Concerning the location error calculation, we applied the method described in Almendros and Chouet (2003), according to which the error in a source position can be defined as the size of the grid region with semblance + R^2 above a certain level. The error estimations were small and generally lower than the grid spacing (250 m).

Regarding volcanic tremor, its temporal variations in terms of source location, amplitude and spectral content were investigated (Figs. 5 and 6). The centroid of the volcanic tremor source was located within 30-min-long non-overlapping sliding windows, filtered in the band 0.5–2.5 Hz, by a grid search method based on the seismic amplitude decay with distance (see Di Grazia et al., 2006 and Cannata et al., 2013, for further details). To take into account only reliable solutions, we accept a location solution only when: i) the goodness of the R^2 fit is higher than 0.9; ii) the number of available stations is higher than 12; and iii) the number of available summit stations is higher than 2. According to the literature, the average location errors, estimated by the

jackknife method (Di Grazia et al., 2006; Cannata et al., 2013), are a few hundred meters in longitude and latitude, and up to 1 km for the altitude (e.g., Patanè et al., 2008; Viccaro et al., 2016; Cannata et al., 2018; Cannavò et al., 2019). Regarding the amplitude, two different estimations were performed. The first, derived from the location algorithm and integrating data from all the above mentioned 16 seismic stations, provided amplitude values reduced at 1 km from the centroid (Fig. 6d). The second consisted of 25° percentile values computed on root mean square (RMS) amplitudes of non-overlapping sliding 10-s-long seismic windows, recorded by ESLN station (see Fig. 1) and filtered in the band 0.5–2.5 Hz. In particular, each percentile value was calculated on 30-min-long windows (Fig. 2b). As for the temporal variation of the spectral content of volcanic tremor, it was estimated by spectra computed on 10.24-s-long sliding windows that do not contain amplitude transients (such as LP events and VT earthquakes). All the spectra falling on the same day were averaged and the average daily spectra were gathered and visualized as a spectrogram (Fig. 6e). In addition, a normalised spectrogram was calculated by dividing each daily spectrum by its maximum value (Fig. 6f).

Finally, visual inspections of the seismic and infrasonic helicorders were performed. In the former case, we looked for clear differences among LP event types, while the latter allowed us to answer the question of whether the LP events showed detectable acoustic components or not. To highlight characteristics of LP events, as well as their eventual acoustic coupling, we plotted in Fig. 7 both waveforms and spectral

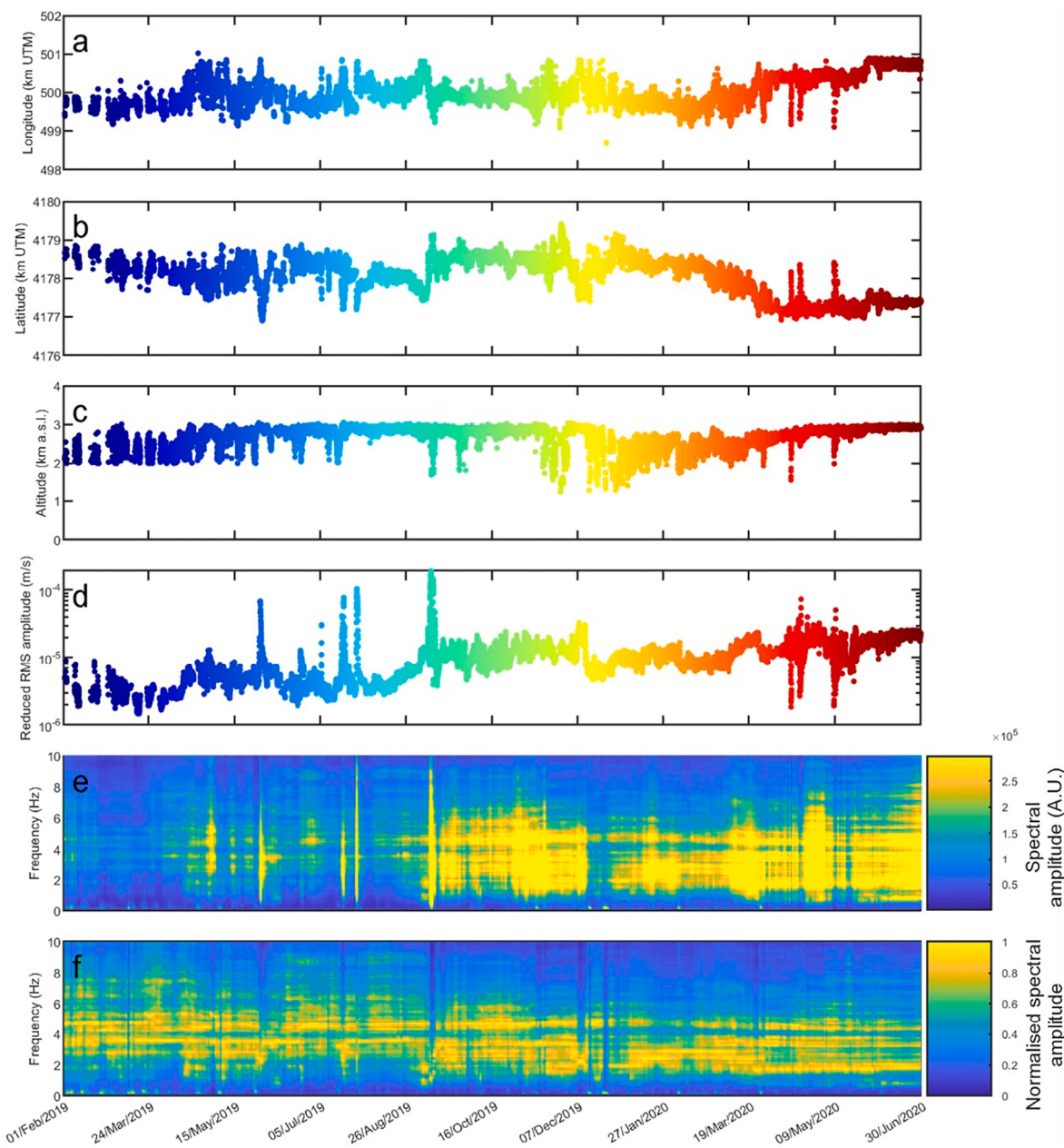


Fig. 6. Variation over time of longitude (a), latitude (b), altitude (c) and 1-km reduced RMS amplitude (d) of the volcanic tremor centroid. Spectrogram (e) and normalised spectrogram (f) computed on the signal recorded by the vertical component of station ECPN.

content of the seismic and infrasonic component of two examples of LP events.

To obtain information about the source mechanisms of both LP events and volcanic tremor, and their prospective differences, scaling relationships have been investigated. In particular, we followed the approaches of previous authors (e.g., Benoit et al., 2003; DeRoin et al., 2015; Sandanbata et al., 2015; Arámbula-Mendoza et al., 2016; Yukutake et al., 2017; Konstantinou et al., 2019), who studied the distribution of duration/number of events versus amplitude of LP seismicity at different volcanoes (Fig. 8). As for the LP events, the scaling relationship was evaluated on the basis of their number and size, estimated as peak-to-peak amplitudes computed at station ESLN (see Fig. 1). Indeed, on the basis of both the distance of ESLN from the LP event sources (~ 6.5 km) and the stability of the LP event source locations, the amplitude variability at such a station well reflects the amplitude variability at the source. In addition, to avoid issues related to the incomplete catalogue of LP events with low amplitudes (it is worth noting that the volcanic

tremor is a continuous background “noise” at Mt. Etna), we took into account only the 50% of the LP events with strongest amplitudes. Indeed, we verified that such an amplitude threshold overcomes the 99° percentile computed on the RMS amplitude time series of the continuous signal (mainly composed of volcanic tremor) acquired by ESLN station. Concerning the volcanic tremor, the scaling relationship was investigated based on the number of 30-min-long windows and the corresponding amplitudes reduced at 1 km from the volcanic tremor source centroid.

3. Results

About 68,000 LP events were detected during February 2019 – June 2020 by STA/LTA algorithm, whose daily number ranged from more than 600 to less than 50 (Fig. 3a). It is worth noting how such a number depends not only on the real LP event occurrence rate, but also on the background “noise” level, that is strongly affected by amplitude

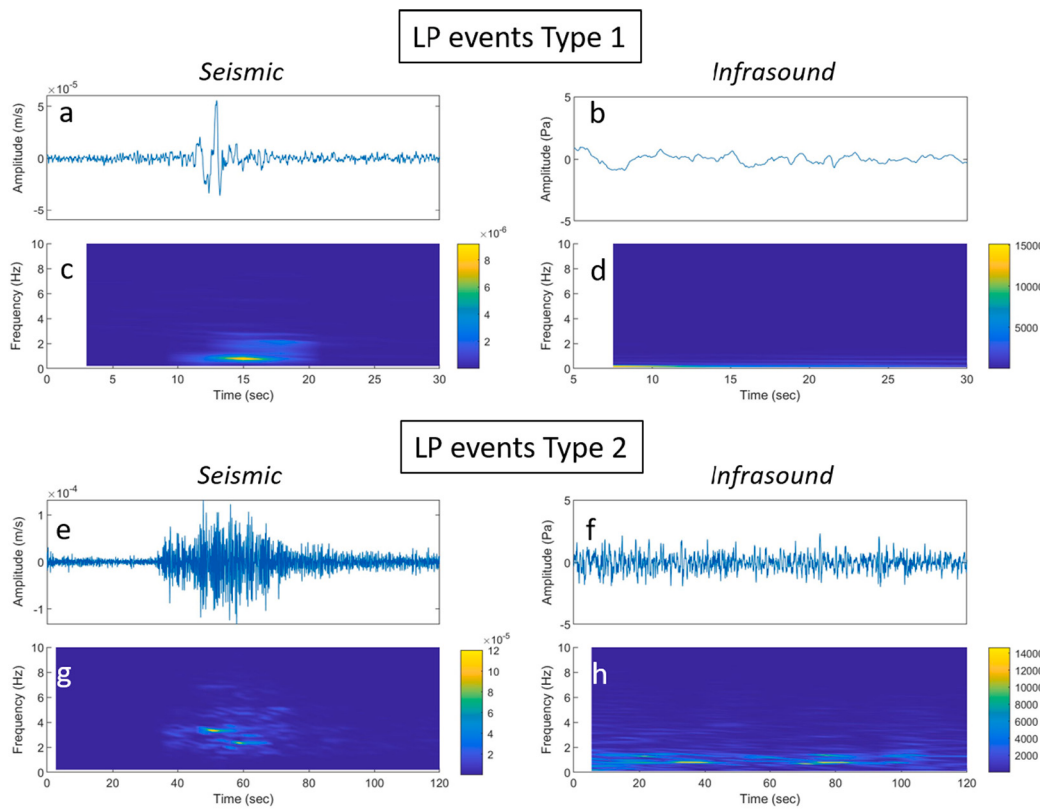


Fig. 7. Seismic (a,e) and infrasonic (b,f) component of LP events Type 1, LP events Type 2 recorded by ECPN station, and corresponding spectrograms (c,d,g,h).

variations of the volcanic tremor. This is also suggested by the plot showing the LP peak-to-peak amplitude over time (Fig. 3b), indicating the near disappearance of weak LP events from October 2019. This change in the LP event behaviour is apparent, because it is related to the increase in volcanic tremor amplitude taking place in September 2019 (Figs. 2b and 6d). On the other hand, some variations of LP activity are reliable, as shown by high LP occurrence rate values observed during periods characterized by medium/high amplitude of volcanic tremor, such as during September 2019. Regarding the peak-to-peak amplitude values as measured by ECPN station, they mostly range between 10^{-5} and 10^{-3} m/s. LP event durations show values from a few seconds to a few tens of seconds (Fig. 3c). In particular, the longest durations were detected during mid-May – mid-June 2019 and March 2020. Regarding the spectral content, most energy is contained in the band 0.5–5.0 Hz. In addition, LP events show intervals with very stable spectral content (with well-defined peak frequencies), as well as periods with sharp or gradual spectral changes (Fig. 3d–g). Similar to the occurrence rate, it is worth noting that also LP spectral content investigation is affected by volcanic tremor. Indeed, while it is possible to precisely identify the spectral content of volcanic tremor (by excluding time windows with amplitude transients), it is not possible to focus only on the spectral contributions of LP events, as volcanic tremor is continuously recorded. This is an issue especially during intervals characterized by high amplitude volcanic tremor. Furthermore, as also highlighted by previous papers (e.g., Patanè et al., 2008, 2013; Cannata et al., 2015), sources of LP events are mostly located below the VOR-BN area at very shallow depths 2.5–3.0 km a.s.l. (Figs. 4 and 5). In addition, the visual inspection of the seismograms allowed identifying a family of LP events (LP events Type 2 in Fig. 7), showing peculiar features, different from the ones characterizing most LP events at Mt. Etna (LP events Type 1 in Fig. 7). These types of events can be distinguished from the other LP events on the basis of their longer duration (Fig. 7e), and peculiar spectral content, dominated by two peaks at 2 and 4 Hz (Fig. 7g). They lack the acoustic component (Fig. 7f, h), and were particularly energetic, in terms of

seismic amplitude, during April 2020 (Fig. 3b). It is worth noting that even Type 1 of LP events lacks a clear acoustic component (Fig. 7b, d).

Concerning volcanic tremor, the amplitudes, as computed 1 km from the source centroid, mostly range from 10^{-6} to 10^{-4} m/s (Fig. 6d). Sharp and short-lived amplitude increases are observed to take place at the same time as explosive activities that occurred on the summit craters (i.e., 30 May, 19 July, 27 July, 10 September 2019, 19 April 2020; Figs. 2b and 6d). In addition, it is also possible to note a longer-lasting increase in volcanic tremor amplitudes, that took place in September 2019 and appears to divide the investigated period into two intervals: i) February–August 2019, showing relatively low volcanic tremor amplitudes; ii) September 2019–June 2020, with higher amplitude values. As for the spectral content, most energy is radiated in the band 1–5 Hz. Similar to LP events, also volcanic tremor shows intervals with stable spectral content and strikingly steady frequency peaks (i.e., 3.7 Hz and 2.1 Hz during February–September 2019 and March–June 2020, respectively), and intervals with changes (Fig. 6e–f). Such steady spectral peaks are also observed at the other stations, thus making us exclude path effects. Concerning the source location of volcanic tremor, similar to LP events, it is mostly located at shallow depth (>1.5 km a.s.l.) below the summit craters. However, unlike LP events, volcanic tremor is characterized by a fairly wide variability of source locations, partly reflecting the spatial evolution of the volcanic activity (Figs. 5 and 6). Indeed, the above-mentioned short-lived amplitude increases are also accompanied by the migration of volcanic tremor source centroid towards the eruptive craters. Moreover, in March 2020 the source centroid moved from the center of the summit area to the NSEC area, and stayed there up to the end of the investigated period.

To better highlight similarities and differences in spectral content of volcanic tremor and LP events, we computed the sum and difference of their normalised spectrograms (Figs. 3g, 6f and 9). In the case of marked spectral similarities between volcanic tremor and LP events, we expect to observe high and low values in the “sum spectrogram” (~2) and “difference spectrogram” (~0), respectively. On the other hand, in the

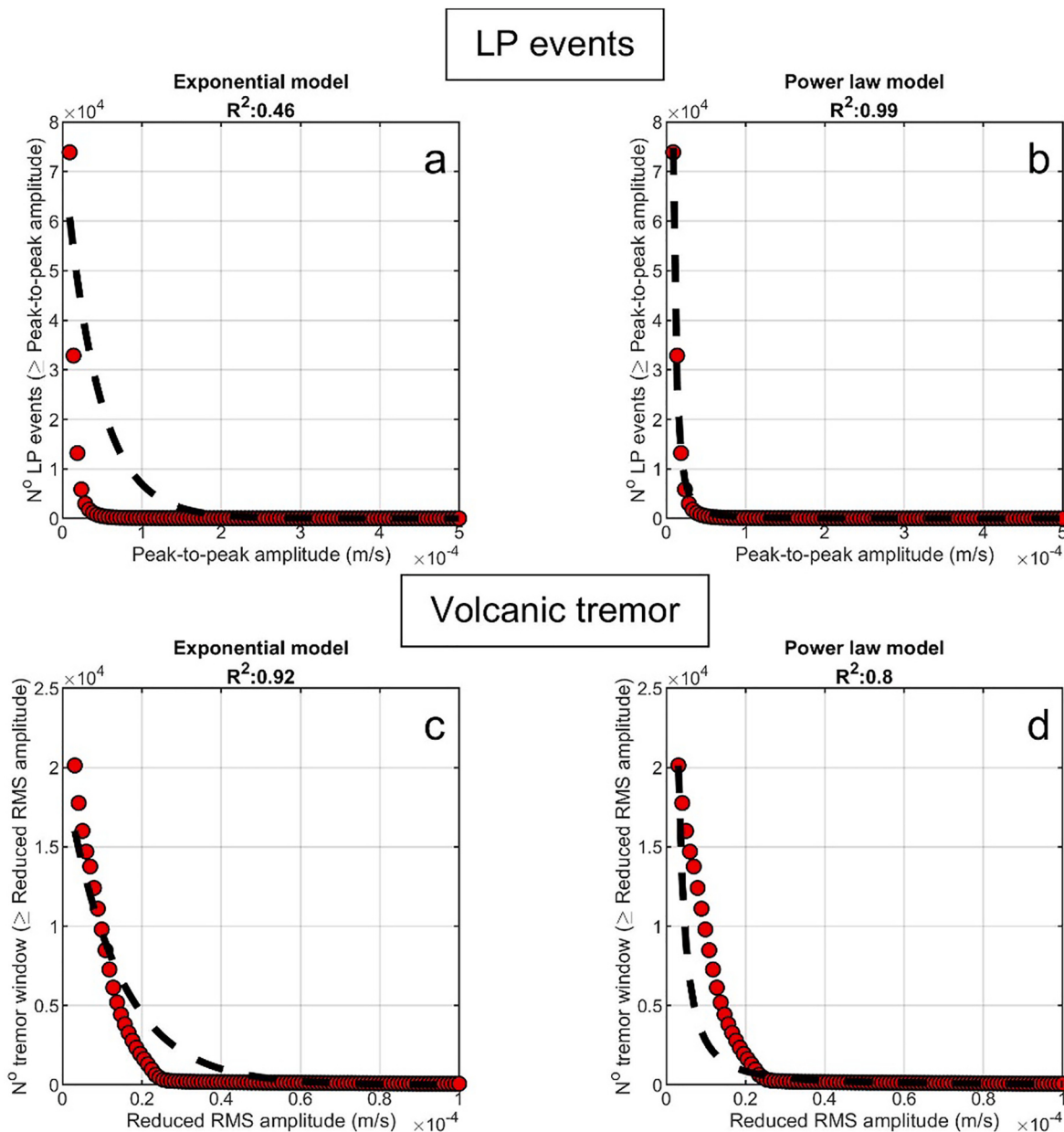


Fig. 8. Comparison between exponential (a,c) and a power law (b,d) scaling models for number of LP events versus peak-to-peak amplitude distribution (a,b) and for number of 30-min-long volcanic tremor windows versus the reduced RMS amplitude (c,d). The red dots show the observed data, while the dashed black lines show the fits to exponential (a,c) and power law (b,d) models. Information about the goodness of exponential and power law fits (R^2 values) are reported in the plot titles. (For interpretation of the references to colour in this figure legend, the reader is referred to the web version of this article.)

case of different frequency contents, low and high (in absolute value) amplitudes are expected in the “sum spectrogram” (~ 0) and “difference spectrogram” ($\sim \pm 1$), respectively (Fig. 9a,b). We focused on the first time interval (February–August 2019), showing relatively low volcanic tremor amplitudes, which allowed us to better distinguish the spectral features of LP events from the ones of volcanic tremor. The LP events turned out to be richer in low frequencies (< 2 Hz) compared to volcanic tremor, as suggested by the high values in the “difference spectrogram”.

Regarding the scaling relationships, Fig. 8 shows that the power law model is a better fit for LP events, while the exponential model for volcanic tremor. Indeed, in the LP event case, the R^2 value is equal to 0.99 and 0.46 for the power law and exponential models, respectively. In the volcanic tremor case, R^2 is 0.8 and 0.92 for the power law and exponential models, respectively.

4. Discussion and conclusions

At some volcanoes, LP events and volcanic tremor have been attributed to the same source mechanism, located in the same volume of the plumbing system, and the latter is considered a coalescence of the former (Latter, 1979; Fehler, 1983; Neuberg, 2011; Hotovec et al., 2012; Chouet and Matoza, 2013). Arguments in support of that mainly rely on three pieces of evidence: i) they share the same spectral content; ii) they are located in the same rock volume; and iii) LP events often increase their occurrence rate and merge into a continuous volcanic tremor. Although this is the most common hypothesis found in literature, studies where this problem has been faced are not many.

Answering this question has direct implications for monitoring and surveillance purposes, as well as for research aims in the field of study of the seismic source mechanisms in volcanic areas. Results of the present

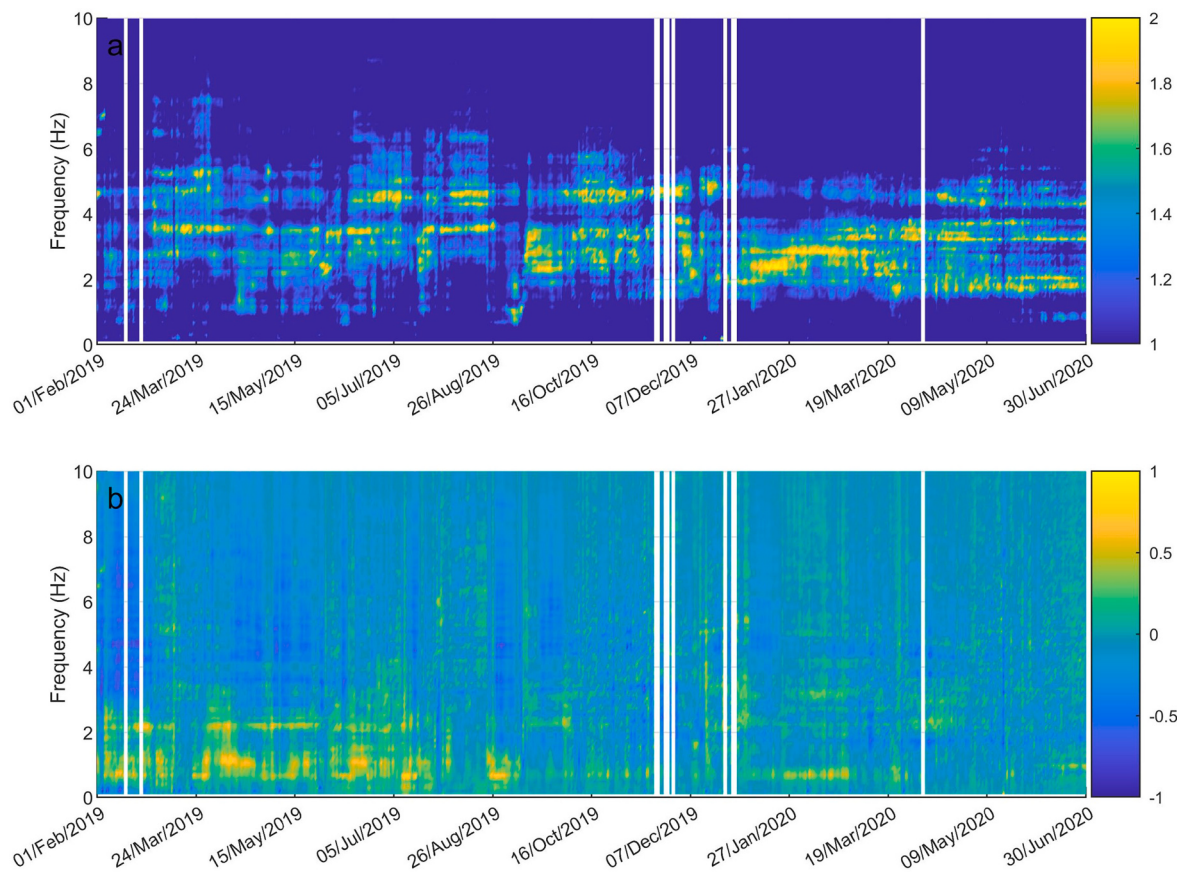


Fig. 9. Sum (a) and difference (b) of the normalised spectrograms of LP events and volcanic tremor, showing similarities and differences in their spectral content.

analysis reveal that this hypothesis is not always valid, or at least suggest that it depends on the volcano taken into account.

Sources of LP events at Etna are mostly located in correspondence of the VOR-BN area at very shallow depths 2.5–3.0 km a.s.l. as shown by this work (Figs. 4 and 5) and also by previous papers dealing with LP events taking place during different time periods (e.g., Patanè et al., 2008, 2013; Cannata et al., 2015). Despite the above-mentioned limitation affecting the detection and characterization of LP events due to the presence of high amplitude volcanic tremor, the source location of LP events stays stable below the VOR-BN area even during the time period September 2019–June 2020, characterized by higher volcanic tremor amplitude. The source location steadiness found in the present work and in the literature, which remains the same even during variations of spectral characteristics of LP events (Patanè et al., 2008, 2013; Cannata et al., 2015), together with the source mechanism invoked to explain their source mechanism at Etna (such as changes in plumbing system state in terms of pressurization), seems to suggest that LP events originate always in the same portion of the shallow plumbing system and are indirectly related to the observable volcanic activity.

Unlike LP events, the source location of volcanic tremor is usually characterized by a fairly wide variability, which reflects both the time evolution of volcanic activity (Figs. 5 and 6) and its location in terms of eruptive vents. Indeed, the short-lived amplitude increases observed during activity intensification are also accompanied by the migration of volcanic tremor source centroids towards the eruptive craters, as occurred, for example, on 30 May and 27–28 July 2019 and in March 2020, when the source centroid moved from the center of the summit area to the NSEC area. Another example is the step-like amplitude increase of the volcanic tremor on 8 September 2019, its sudden migration towards NEC area and its successive shift towards the location it had before 8 September 2019. In other words, the volcanic tremor becomes stronger beneath the vents just before they erupt.

The spectral contents of LP events and volcanic tremor show differences. Indeed, focusing on the first time interval (February–August 2019) showing relatively low volcanic tremor amplitudes, the LP events (regardless the LP type taken into account) turned out to be richer in low frequencies (<2 Hz) compared to volcanic tremor (Figs. 3g, 6f and 9).

The different behaviour of volcanic tremor and LP events at Mt. Etna is also confirmed by the different scaling laws explaining the distributions duration/number of events versus size (Fig. 8). Indeed, the exponential model is a better fit for the volcanic tremor, in agreement with observations collected in other volcanoes and geothermal areas (e.g., Benoit et al., 2003; Yukutake et al., 2017; Konstantinou et al., 2019). Hence, the source process of volcanic tremor at Mt. Etna should be scale bound, not scale invariant (Benoit et al., 2003). On the basis of previous studies (Benoit et al., 2003; Yukutake et al., 2017), such a scale bound process could be characterized by a fixed geometry, related to the structure of the upper portion of the plumbing system (fixed characteristic length or scale), with variable forces exciting the volcanic tremor radiation, that could be interpreted as resulting from the flow of fluids along such a plumbing system portion. On the other hand, the number of LP events versus size distribution is better explained by a power law. Such a relationship (also indicated as fractal scaling, self-similar, or scale invariant; e.g. Benoit et al., 2003), fairly common in natural processes such as tectonic earthquakes (Gutenberg and Richter, 1954), volcanic eruptions (Simkin, 1993) and dike intrusion processes (Passarelli et al., 2014), was also found suited to explain the size-frequency distribution of volcanic explosion earthquakes (Nishimura and Hamaguchi, 1993; Nishimura et al., 2016) and B-type volcanic earthquakes (Minakami, 1960). It implies that the source has no characteristic scale and hence is self-similar.

Finally, from time series analyses, in particular from LP occurrence rates and amplitudes, and volcanic tremor amplitude, emerges that they exhibit different trends during the analysed period. Focusing on

amplitude, while the LP highest amplitudes were observed during February, mid-August - mid-September 2019 and April 2020, volcanic tremor amplitude was on a low level in the first case and on a medium-high level in the second and third cases (Figs. 3b and 6d). From a volcanological point of view the period February–May 2019 was characterized by no significant volcanic activity. Volcanic tremor amplitude seems to be more closely correlated with volcanic activity than LP event amplitude (Figs. 2b and 6d). Indeed, starting from May 2019, when a weak volcanic tremor amplitude increase was observed, lava effusion and Strombolian activity resumed from SEC/NSEC craters and punctual ash emission from NEC occurred. Later on, in September 2019, in concomitance with a more evident increase of volcanic tremor amplitude, continuous Strombolian activity started at VOR, and from December ash emission alternated with Strombolian activity were continuously observed in the SEC/NSEC area.

The above reported evidence leads us towards the hypothesis that LP events and volcanic tremor at Mt. Etna are not due to a common source mechanism, but rather to two different processes. While the volcanic tremor source mechanism is a scale bound process directly linked to the observable changes in the eruptive activities, LP event source is better described by a scale invariant process not so directly related to the variations in the eruptive activities.

A clarification needs to be made about the possibility of extending the result of our analysis to other volcanoes. The hypothesis of different source mechanisms for the two types of seismo-volcanic signals, formulated for Etna volcano, has also been advanced at Arenal volcano (Almendros et al., 2014). However, it can be invalid for other volcanic areas. Indeed, it has to be mentioned that LP events and volcanic tremor are produced by multiple volcanic phenomena, which can vary at the different volcanoes and, more important, their characteristics are function of the amount/characteristics of fluids and the shallow plumbing system conditions.

It is worth noting that volcanoes where these two signals have been associated to the same source mechanism exhibit different eruptive style from Etna, such as for example Popocatepetl (Arciniega-Ceballos et al., 2000), Soufriere Hills and Galeras (Neuberg, 2011).

Therefore, we believe that the hypothesis that volcanic tremor is made up by a superimposition of very close in time LP events, as well as our opposite inference, cannot be considered a generalization. This issue is relevant in the perspective of volcano monitoring and surveillance and hence needs in depth investigations.

Author contribution

All the authors initiated the concept of the paper. MS, AC and GDG performed formal data analysis. MS and AC wrote the draft of the paper. GDG and PM dealt with data curation and contributed to the editing of the manuscript. All the author participated to the interpretation and discussion of the results.

Declaration of Competing Interest

The authors declare that they have no known competing financial interests or personal relationships that could have appeared to influence the work reported in this paper.

Acknowledgements

We are indebted to the technicians of the INGV, Osservatorio Etneo for enabling the acquisition of seismic and infrasonic data. A.C. thanks CHANCE project, II Edition, Università degli Studi di Catania (principal investigator A. Cannata) and grant PIACERI, 2020-22 programme (PAROSSIMA project, code 22722132140; principal investigator Marco Viccaro).

References

- Aki, K., Richards, P.G., 2002. Quantitative Seismology, Second edition. University Science Books, Sausalito, California.
- Almendros, J., Chouet, B., 2003. Performance of the radial semblance method for the location of very long period volcanic signals. Bull. Seismol. Soc. Am. 93 (5), 1890–1903. <https://doi.org/10.1785/0120020143>.
- Almendros, J., Abella, R., Mora, M.M., Lesage, P., 2014. Array analysis of the seismic wavefield of long-period events and volcanic tremor at Are-nal volcano, Costa Rica. J. Geophys. Res. Solid Earth 119, 5536–5559. <https://doi.org/10.1002/2013JB010628>.
- Alparone, S., Cannata, A., Gresta, S., 2007. Time variation of spectral and wavefield features of volcanic tremor at Mt. Etna (January–June 1999). J. Volcanol. Geotherm. Res. 161, 318–332. <https://doi.org/10.1016/j.jvolgeores.2006.12.012>.
- Andronico, D., Cannata, A., Di Grazia, G., Ferrari, F., 2021. The 1986–2021 paroxysmal episodes at the summit craters of Mt. Etna: insights into volcano dynamics and hazard. Earth Sci. Rev. 103686. <https://doi.org/10.1016/j.earscirev.2021.103686>.
- Arámbula-Mendoza, R., Valdés-González, C., Varley, N., Reyes-Pimentel, T.A., Juárez-García, B., 2016. Tremor and its duration-amplitude distribution at Popocatépetl volcano, Mexico. Geophys. Res. Lett. 43, 8994–9001. <https://doi.org/10.1002/2016GL070227>.
- Arciniega-Ceballos, A., Valdes, C., Dawson, P., 2000. Temporal and spectral characteristics of seismicity observed at Popocatépetl volcano, Central Mexico. J. Volcanol. Geotherm. Res. 102, 207–216. [https://doi.org/10.1016/S0377-0273\(00\)00188-8](https://doi.org/10.1016/S0377-0273(00)00188-8).
- Bean, C.J., De Barros, L., Lokmer, I., Métaxian, J.P., O'Brien, G.S., Murphy, S., 2014. Long-period seismicity in the shallow volcanic edifice formed from slow-rupture earthquakes. Nat. Geosci. 7, 71–75. <https://doi.org/10.1038/ngeo2027>.
- Benoit, J.P., McNutt, S.R., Barboza, V., 2003. Duration-amplitude distribution of volcanic tremor. J. Geophys. Res. 108 (B3), 2146. <https://doi.org/10.1029/2001JB001520>.
- Bonforte, A., Guglielmino, F., Puglisi, G., 2019. Large dyke intrusion and small eruption: the December 24, 2018 Mt. Etna eruption imaged by Sentinel-1 data. Terra Nova 31 (4), 405–412. <https://doi.org/10.1111/ter.12403>.
- Buurman, H., West, M.E., 2010. Seismic precursors to volcanic explosions during the 2006 eruption of Augustine Volcano. In: Power, J.A., Coombs, M.L., Freymueller, J.T. (Eds.), The 2006 eruption of Augustine Volcano: U.S. Geological Survey Professional Paper 1769, Menlo Park, CA, pp. 41–57.
- Buurman, H., West, M.E., Thompson, G., 2013. The seismicity of the 2009 Redoubt eruption. J. Volcanol. Geotherm. Res. 259, 16–30. ISSN 0377-0273. <https://doi.org/10.1016/j.jvolgeores.2012.04.024>.
- Calvari, S., Bilotta, G., Bonaccorso, A., Caltabiano, T., Cappello, A., Corradino, C., Spampinato, L., 2020. The VEI 2 Christmas 2018 Etna eruption: a small but intense eruptive event or the starting phase of a larger one? Remote Sens. 12 (6), 905.
- Cannata, A., Di Grazia, G., Montalto, P., Ferrari, F., Nunzari, G., Patanè, D., Privitera, E., 2010. New insights into banded tremor from the 2008–2009 Mount Etna eruption. J. Geophys. Res. Solid Earth 115 (B12). <https://doi.org/10.1029/2009JB007120>.
- Cannata, A., Di Grazia, G., Aliotta, M., Cassisi, C., Montalto, P., Patanè, D., 2013. Monitoring seismo-volcanic and infrasonic signals at volcanoes: Mt. Etna case study. Pure Appl. Geophys. 170, 1751–1771. <https://doi.org/10.1007/s00024-012-0634-x>.
- Cannata, A., Spedalieri, G., Behncke, B., Cannavò, F., Di Grazia, G., Gambino, S., Gresta, S., Gurrieri, S., Liuzzo, M., Palano, M., 2015. Pressurization and depressurization phases inside the plumbing system of Mount Etna volcano: evidence from a multiparametric approach. J. Geophys. Res. Solid Earth 120. <https://doi.org/10.1002/2015JB012227>.
- Cannata, A., Di Grazia, G., Giuffrida, M., Gresta, S., Palano, M., Sciotto, M., et al., 2018. Space-time evolution of magma storage and transfer at Mt. Etna volcano (Italy): the 2015–2016 reawakening of Voragine crater. Geochim. Geophys. Geosyst. 19. <https://doi.org/10.1002/2017GC007296>.
- Cannavò, F., Cannata, A., Cassisi, C., Di Grazia, G., Montalto, P., Prestifilippo, M., Privitera, E., Coltellini, M., Gambino, S., 2017. A multivariate probabilistic graphical model for real-time volcano monitoring on Mount Etna. J. Geophys. Res. Solid Earth 122, 3480–3496. <https://doi.org/10.1002/2016JB013512>.
- Cannavò, F., Sciotto, M., Cannata, A., Di Grazia, G., 2019. An integrated geophysical approach to track magma intrusion: the 2018 Christmas eve eruption at Mt. Etna. Geophys. Res. Lett. 46. <https://doi.org/10.1029/2019GL083120>.
- Carniel, R., Del Pin, E., Budai, R., Pascolo, P., 2005. Identifying timescales and possible precursors of the awake to asleep transition in EOG time series. Chaos Solit. Fract. 23, 1259–1266. <https://doi.org/10.1016/j.chaos.2004.06.021>.
- Chouet, B., 1996. Long-period volcano seismicity: its source and use in eruption forecasting. Nature 380, 309–316. <https://doi.org/10.1038/380309a0>.
- Chouet, B.A., Matiza, R.S., 2013. A multi-decadal view of seismic methods for detecting precursors of magma movement and eruption. J. Volcanol. Geotherm. Res. 252, 108–175. <https://doi.org/10.1016/j.jvolgeores.2012.11.013>.
- Chouet, B.A., Page, R.A., Stephens, C.D., Lahr, J.C., Power, J.A., 1994. Precursory swarms of long-period events at Redoubt Volcano (1989–1990), Alaska: their origin and use as a forecasting tool. J. Volcanol. Geotherm. Res. 62 (1), 95–135. [https://doi.org/10.1016/0377-0273\(94\)90030-2](https://doi.org/10.1016/0377-0273(94)90030-2).
- Chouet, B., Dawson, P., Ohminato, T., Martini, M., Saccorotti, G., Giudicepietro, F., Scarpa, R., 2003. Source mechanisms of explosions at Stromboli Volcano, Italy, determined from moment-tensor inversions of very-long-period data. J. Geophys. Res. Solid Earth 108 (B1), ESE-7.
- D'Agostino, M., Di Grazia, G., Ferrari, F., Langer, H., Messina, A., Reitano, D., Spampinato, S., 2013. Volcano Monitoring and Early Warning on Mt Etna Based on Volcanic Tremor—Methods and Technical Aspects. chap. 4. NOVA Science Publ, New York, pp. 53–92.

- D'Auria, L., Barrancos, J., Padilla, G.D., Pérez, N.M., Hernández, P.A., Melián, G., et al., 2019. The 2016 Tenerife (Canary Islands) long-period seismic swarm. *J. Geophys. Res. Solid Earth* 124, 8739–8752. <https://doi.org/10.1029/2019JB017871>.
- DeRoin, N., McNutt, S., Thompson, G., 2015. Duration-amplitude relationships of volcanic tremor and earthquake swarms preceding and during the 2009 eruption of Redoubt Volcano, Alaska. *J. Volcanol. Geotherm. Res.* 292, 56–69. <https://doi.org/10.1016/j.jvolgeores.2015.01.003>.
- Di Grazia, G., Falsaperla, S., Langer, H., 2006. Volcanic tremor location during the 2004 Mount Etna lava effusion. *Geophys. Res. Lett.* 33, L04304. <https://doi.org/10.1029/2005GL025177>.
- Fehler, M., 1983. Observations of volcanic tremor at Mount St. Helens volcano. *J. Geophys. Res.* 88, 3476–3484. <https://doi.org/10.1029/JB088iB04p03476>.
- Fujita, E., 2008. Banded tremor at Miyakejima volcano, Japan: implication for two-phase flow instability. *J. Geophys. Res. Solid Earth* 113 (B4). <https://doi.org/10.1029/2006JB004829>.
- Gestrich, J.E., Fee, D., Tsai, V.C., Haney, M.M., Van Eaton, A.R., 2020. A physical model for volcanic eruption tremor. *Journal of geophysical research: solid Earth* 125 (10). <https://doi.org/10.1029/2019JB018980> e2019JB018980.
- Girona, T., Caudron, C., Huber, C., 2019. Origin of shallow volcanic tremor: the dynamics of gas pockets trapped beneath thin permeable media. *J. Geophys. Res. Solid Earth* 124 (5), 4831–4861. <https://doi.org/10.1029/2019JB017482>.
- Giuffrida, M., Scandura, M., Costa, G., Zuccarello, F., Sciotto, M., Cannata, A., Viccaro, M., 2021. Tracking the summit activity of Mt. Etna volcano between July 2019 and January 2020 by integrating petrological and geophysical data. *J. Volcanol. Geotherm. Res.* 418 <https://doi.org/10.1016/j.jvolgeores.2021.107350>, 107350.
- Global Volcanism Program, 2013. Volcanoes of the World, v. 4.10.3 (15 Oct 2021).
- Venzke, E. (ed.), Smithsonian Institution. <https://doi.org/10.5479/si.GVP.VOTW4-2013>. Downloaded 03 Dec 2021.
- Gresta, S., Montalto, A., Patanè, G., 1991. Volcanic tremor at Mt. Etna (January 1984–March 1985): its relationship to the eruptive activity and modelling of the summit feeding system. *Bull. Volcanol.* 53, 309–320. <https://doi.org/10.1007/BF00414527>.
- Gutenberg, B., Richter, C.F., 1954. Magnitude and energy of earthquakes. *Ann. Geofis.* 9, 1–15. <https://doi.org/10.4401/ag-5590>.
- Haney, M.M., Fee, D., McKee, K.F., Lyons, J.J., Matoza, R.S., et al., 2020. Co-eruptive tremor from Bogoslof volcano: seismic wavefield composition at regional distances. *Bull. Volcanol.* 82 (2), 1–14. <https://doi.org/10.1007/s00445-019-1347-0>.
- Hotovec, A.J., Prejean, S.G., Vidale, J.E., Gomberg, J., 2012. Strongly gliding harmonic tremor during the 2009 eruption of Redoubt Volcano. *J. Volcanol. Geotherm. Res.* <https://doi.org/10.1016/j.jvolgeores.2012.01.001>.
- Ichihara, M., 2016. Seismic and infrasonic eruption tremors and their relation to magma discharge rate: a case study for sub-Plinian events in the 2011 eruption of Shinmoedake, Japan. *J. Geophys. Res. Solid Earth* 121 (10), 7101–7118. <https://doi.org/10.1002/2016JB013246>.
- Konstantinou, K.I., Astrid Ardiani, M., Sudiby, M.R.P., 2019. Scaling behavior and source mechanism of tremor recorded at Erebus volcano, Ross island, Antarctica. *Phys. Earth Planet. Inter.* 290, 99–106. <https://doi.org/10.1016/j.pepi.2019.03.010>.
- Lahr, J.C., Chouet, B.A., Stephens, C.D., Power, J.A., Page, R.A., 1994. Earthquake classification, location, and error analysis in a volcanic environment: implications for the magmatic system of the 1989–1990 eruptions at redoubt volcano, Alaska. *J. Volcanol. Geotherm. Res.* 62 (1–4), 137–151. [https://doi.org/10.1016/0377-0273\(94\)90031-0](https://doi.org/10.1016/0377-0273(94)90031-0).
- Latter, J., 1979. Volcanological observations at Tongariro national park. 2: types and classification of volcanic earthquakes 1976–1978. *Geophys. Div. Rep.* 150, IV–60. Dept. Sci. Ind. Res.
- McNutt, S., 2005. Volcanic seismology. *Annu. Rev. Earth Planet. Sci.* 32, 461–491. <https://doi.org/10.1146/annurev.earth.33.092203.122459>.
- McNutt, S.R., Roman, D.C., 2015. Volcanic seismicity. In: McNutt, S.R., Houghton, B., Stix, J., Rymer, H., Sigurdsson, H. (Eds.), *The Encyclopedia of Volcanoes*. Elsevier. <https://doi.org/10.1016/B978-0-12-385938-9.00059-6>.
- Minakami, T., 1960. Fundamental research for predicting volcanic eruptions. *Bull. Earth Res. Inst.* 38, 497–544.
- Neidell, N., Taner, M.T., 1971. Semblance and other coherency measures for multichannel data. *Geophysics* 36, 482–497. <https://doi.org/10.1190/1.1440186>.
- Neri, M., Maio, M.D., Crepaldi, S., Suozzi, E., Lavy, M., Marchionatti, F., et al., 2017. Topographic maps of Mount Etna's summit craters, updated to December 2015. *Journal of Maps* 13 (2), 674–683. <https://doi.org/10.1080/17445647.2017.1352041>.
- Neuberg, J.W., 2011. Earthquakes, volcanogenic. In: Gupta, H.K., et al. (Eds.), *Encyclopedia of Solid Earth Geophysics*. Springer, pp. 261–269 doi: 10.1007/978-90-481-8702-7_159.
- Nishimura, T., Hamaguchi, H., 1993. Scaling law of volcanic explosion earthquake. *Geophys. Res. Lett.* 20 (22), 2479–2482. <https://doi.org/10.1029/93GL02793>.
- Nishimura, T., Iguchi, M., Hendrasto, M., Aoyama, H., Yamada, T., Ripepe, M., Genco, R., 2016. Magnitude–frequency distribution of volcanic explosion earthquakes. *Earth, Planets and Space* 68 (1), 1–12. <https://doi.org/10.1186/s40623-016-0505-2>.
- Passarelli, L., Rivalta, E., Shuler, A., 2014. Dike intrusions during rifting episodes obey scaling relationships similar to earthquakes. *Sci. Rep.* 4, 3886. <https://doi.org/10.1038/srep03886>.
- Patanè, D., Di Grazia, G., Cannata, A., Montalto, P., Boschi, E., 2008. Shallow magma pathway geometry at Mt. Etna volcano. *Geochem. Geophys. Geosyst.* 9, 12. <https://doi.org/10.1029/2008GC002131>.
- Patanè, D., Aiuppa, A., Aloisi, M., Behncke, B., Cannata, A., Coltellini, M., Di Grazia, G., et al., 2013. Insights into magma and fluid transfer at Mount Etna by a multiparametric approach: a model of the events leading to the 2011 eruptive cycle. *J. Geophys. Res. Solid Earth* 118 (7), 3519–3539. <https://doi.org/10.1002/jgrb.50248>.
- Potter, S.H., Jolly, G.E., Neall, V.E., Johnston, D.M., Scott, B.J., 2014. Communicating the status of volcanic activity: revising New Zealand's volcanic alert level system. *J. Appl. Volcanol.* 3, 1–16. <https://doi.org/10.1186/s13617-014-0013-7>.
- Sandanbata, O., Obara, K., Maeda, T., Takagi, R., Satake, K., 2015. Sudden changes in the amplitude–frequency distribution of long-period tremors at Aso volcano, Southwest Japan. *Geophys. Res. Lett.* 42, 10,256–10,262. <https://doi.org/10.1002/2015GL066443>.
- Simkin, T., 1993. Terrestrial volcanism in space and time. *Annu. Rev. Earth Planet. Sci.* 21, 427–452. <https://doi.org/10.1146/annurev.ea.21.050193.002235>.
- Spina, L., Cannata, A., Privitera, E., Vergniolle, S., Ferlito, C., Gresta, S., Montalto, P., Sciotto, M., 2014. Insights into Mt. Etna's shallow plumbing system from the analysis of infrasound signals, August 2007–December 2009. *Pure Appl. Geophys.* 172, 473–490. <https://doi.org/10.1007/s0024-014-0884-x>.
- Trmkoczy, A., 2012. Understanding and parameter setting of STA/LTA trigger algorithm. In: Bormann, P. (Ed.), *IASPEI New Manual of Seismological Observatory Practice 2 (NMSOP-2)*. IASPEI, Potsdam, pp. 1–20. https://doi.org/10.2312/GFZ.NMSOP-2_IS_8.1.
- Viccaro, M., Zuccarello, F., Cannata, A., Palano, M., Gresta, S., 2016. How a complex basaltic volcanic system works: constraints from integrating seismic, geodetic, and petrological data at Mount Etna volcano during the July–August 2014 eruption. *J. Geophys. Res. Solid Earth* 121, 5659–5678. <https://doi.org/10.1002/2016JB013164>.
- Wassermann, J., 2012. In: Bormann, P. (Ed.), *Volcano Seismology, IASPEI New Manual of Seismological Observatory Practice 2 (NMSOP-2)*, 2nd ed. Deutsches GeoForschungsZentrum GFZ, Potsdam, Potsdam, pp. 1–77. <https://doi.org/10.2312/GFZ.NMSOP-2.ch13>.
- Yukutake, Y., Honda, R., Harada, M., Doke, R., Saito, T., Ueno, T., Sakai, S., Morita, Y., 2017. Analyzing the continuous volcanic tremors detected during the 2015 phreatic eruption of the Hakone volcano. *Earth, Planets and Space* 69, 164. <https://doi.org/10.1186/s40623-017-0751-y>.
- Zobin, V.M., 2012. *Introduction to Volcanic Seismology*, Second Ed. Elsevier. <https://doi.org/10.1016/C2011-0-06141-0>.